resources

MDPI

Article

Multiobjective Optimisation of Flotation Variables Using Controlled-NSGA-II and Paretosearch

Bismark Amankwaa-Kyeremeh [1], Conor McCamley [2], Kathy Ehrig [3] and Richmond K. Asamoah [1,*]

[1] Future Industries Institute, University of South Australia, Mawson Lakes, Adelaide, SA 5095, Australia
[2] Syrah Resources, Melbourne, VIC 3000, Australia
[3] BHP Olympic Dam, Adelaide, SA 5000, Australia
* Correspondence: richmond.asamoah@unisa.edu.au

Abstract: Finding the optimum operating points for the maximisation of flotation recovery and concentrate grade can be a very difficult task, owing to the inverse relationship that exists between these two key performance indicators. For this reason, techniques that can accurately find the trade-off are critical for flotation process optimisation. This work extracted well-assessed Gaussian process predictive functions as objective functions for a comparative multiobjective optimisation study using the paretosearch algorithm (PA) and the controlled elitist non-dominated sorting genetic algorithm (controlled-NSGA-II). The main aim was the concomitant maximisation of the copper recovery and the concentrate grade. Comparison of the two applied techniques revealed that the PA discovered the best set of the pareto-optimal solution for both the recovery (93.4%) and concentrate-grade (17.4 wt.%) maximisation.

Keywords: paretosearch algorithm; controlled-NSGA-II; ore variability; flotation copper recovery and grade; multiobjective optimisation

check for updates

Citation: Amankwaa-Kyeremeh, B.; McCamley, C.; Ehrig, K.; Asamoah, R.K. Multiobjective Optimisation of Flotation Variables Using Controlled-NSGA-II and Paretosearch. *Resources* **2024**, *13*, 157. https://doi.org/10.3390/resources13110157

Academic Editor: Benjamin McLellan

Received: 22 May 2024
Revised: 6 October 2024
Accepted: 31 October 2024
Published: 7 November 2024

1. Introduction

Flotation modelling has received much attention since the early 1930s and can be classified into different categories based on its characteristics and usage. For instance Gharai and Venugopal [1] classified flotation models into macro-scale and micro-scale based on the overall process and subprocesses occurring in a flotation system. According to their classification, the micro-scale looks at the chemical and physical correlation among subprocesses in a flotation cell, while the macro-scale is the simplification and combination of a number of micro-scale models for the prediction of the overall behaviour of a flotation cell or even banks [2]. Another classification performed by Quintanilla, Neethling [3] distinguished flotation models into models for simulation purposes and models for control purposes. Despite the numerous models developed under the various classifications highlighted above, froth flotation modelling has always been a difficult task due to the complex nonlinear dynamic nature of the various process variables. The complex nonlinear relationships existing among the flotation variables have presented significant reliability and utilisation challenges for traditional first-principle models (e.g., first-order kinetic approach), which may involve some assumptions [4–8].

With the inability of conventional models like empirical or phenomenological models to fully capture these complex nonlinear relationships, attention has been drawn to modern day machine learning (supervised and unsupervised) algorithms in modelling froth flotation outcomes. Machine learning algorithms, if properly trained with a high-quality data set, have the ability to capture variable relationships for predicting the outcome of a future unseen data set. Commonly applied machine learning algorithms in the modelling of the metallurgical performance of froth flotation include fuzzy logic, support vector machine, decision trees, principal component regression, random forest, and artificial neural network [9–15]. In recent times, application of a probabilistic Gaussian process

regression (GPR) algorithm has acquired much attention over most nonlinear modelling techniques [16]. The successful application of the GPR algorithm in the field of particle separation includes recent work where the flotation recovery was predicted from model-selected flotation variables [17,18]. Another success story of the GPR algorithm in the field of minerals engineering was its application by Patel, Gorai [19] in predicting the iron ore grade from image analysis. The main advantage of the GPR algorithm is its ability to include prior knowledge of the noise in the measured data in the model [20]. Previous publications have compared different machine learning model performances; hence, this will not be repeated here [21–23].

Once a machine learning algorithm is well-trained with good prediction accuracy, its predictive function can be used for process optimisation [24]. In machine learning process optimisation, optimal operating points of process variables are ascertained for peak performance after modelling the key performance indicators with other process variables [25,26]. Over the years, several optimisation algorithms including particle swarm optimisation, ant colony algorithm, gravitational search algorithm, evolutionary algorithm, genetic algorithm, simulated annealing, surrogate optimisation, and tabu search have been developed, with regard to recent emerging advanced computational techniques [27]. While some optimisation problems may just involve one goal, some real-life situations like froth flotation require more than one goal to be achieved simultaneously, and therefore, there is a need for multiobjective optimisation (MO) techniques. MO is an enterprising area of research, which has gained much attention in many scientific and engineering fields [28]. MO allows decisionmakers to plan and make decisions with multiple conflicting or sometimes nonconflicting goals.

The conventional approach for solving MO problems has been the use of scalarisation techniques, converting MO to single-objective problems. With these single objective-based techniques, only a single solution is found, leaving multiobjective problems partially solved and incomplete. Several multiobjective evolutionary algorithms (MOEAs) such as the non-dominated sorting genetic algorithm (NSGA) address this problem; however, it suffers from a lack of elitism, high computational complexity, and the requirement for a sharing-parameter σ_{share} specification. As a result, an improved, elitist-NSGA (NSGA-II) was proposed and shown to perform better than other elitist MOEAs (e.g., pareto archive evolution strategy (PAES) and strength pareto evolution algorithm (SPEA)) in finding diverse solutions and in converging close to the true (actual) pareto-optimal set. These results encourage the application of NSGA-II to more complex real-life MO problems [29,30]. Irrespective of the numerous applications of NSGA-II, it had the issue of premature convergence to a suboptimal solution set, and as such, the proposal of the controlled-NSGA-II comes with controlled elitism for better convergence performance. Another powerful MO technique is the paretosearch algorithm (PA). PA was applied by Gantayet and Dheer [31] in finding the optimal planning strategy for a radial distribution network. Mišo, Branko [32] also applied PA for the multiobjective calibration in a gas–metal arc welding process simulation [33].

In this work, a comparative MO study has been carried out on various rougher flotation variables using the PA and controlled-NSGA-II following a Gaussian process prediction of both copper recovery and the copper concentrate grade. The work aimed at finding the optimum operating points of various rougher flotation variables for the maximisation of both the copper recovery and the concentrate copper grade. PA and controlled-NSGA-II have not been applied in any flotation variables optimisation study previously. A paucity of information exists on the use of the predictive functions of a GPR model as the objective functions for the multiobjective optimisation of industrial flotation variables. Another unique thing about this work is that effort has been made to select the best pareto-optimal solution, a difficult decision to make in MO problems.

2. Research Methodology

This section specifically captures the data collection and pre-processing, predictive model development and assessment, theoretical overview of MO algorithms, and finally, optimisation modelling. A detailed theoretical overview of the GPR algorithm has been presented elsewhere and will not be repeated here [17,20]. MATLAB R2020b (64-bit version) was used for the various algorithm implementations.

2.1. Data Collection and Pre-Processing

A total of 80,000 data observations were collected from the copper mineral (e.g., chalcopyrite and bornite) flotation circuit, specifically the rougher circuit. The extracted data include variables such as ore feed grade, mill throughput, hydrocyclone overflow particle percent passing the 75 µm size, xanthate dosage (tank 1 and 4), frother dosage (tank 1 and 4), airflow rate (tank 1, 2, 3, 4, and 5), and froth depth (tank 1, 2, and 4). These flotation variables are the main variables that are known to enhance both the rougher copper recovery and grade and whose optimisation was of much interest to the metallurgist. All the variables are monitored directly and independently except for the rougher copper recovery, which is estimated from onstream analyser (OSA) readings from rougher feed, cleaner concentrate, and scavenger tails using Equation (1). Furthermore, Ehrig, McPhie [34] have provided more details about the deposit mineralisation. Details of the rougher flotation circuit under consideration have been previously presented. The data preprocessing are consistent with the previous publications, including domain knowledge for outlier removal and data standardisation [17].

$$\text{Recovery } R_i = \left(\frac{c_i}{f_i}\right)\left(\frac{f_{i-t_i}}{c_{i-t_i}}\right) \times 100\%,\ i = 1, 2, 3, \ldots, \tag{1}$$

where

$c_i = i$th concentrate grade;
$f_i = i$th feed grade;
$t_i = i$th tails grade.

The essence of the standardisation is to reduce the impact of the variables with high variance and of different scales or magnitude on the model prediction outcomes. For confidentiality reasons, only standardised results are presented in this work. Equation (2) shows the equation for standardisation. Figure 1 is a visualisation of the variation in the output variables and some input variables.

$$Z_i = \frac{a_i - \overline{a}_i}{\sigma_a},\ i = 1, 2, 3, \ldots, \tag{2}$$

where

Z_i = transformed observation;
a_i = observation of variable a;
$\overline{a}_i$ = mean of variable a;
σ_i = standard deviation of variable a.

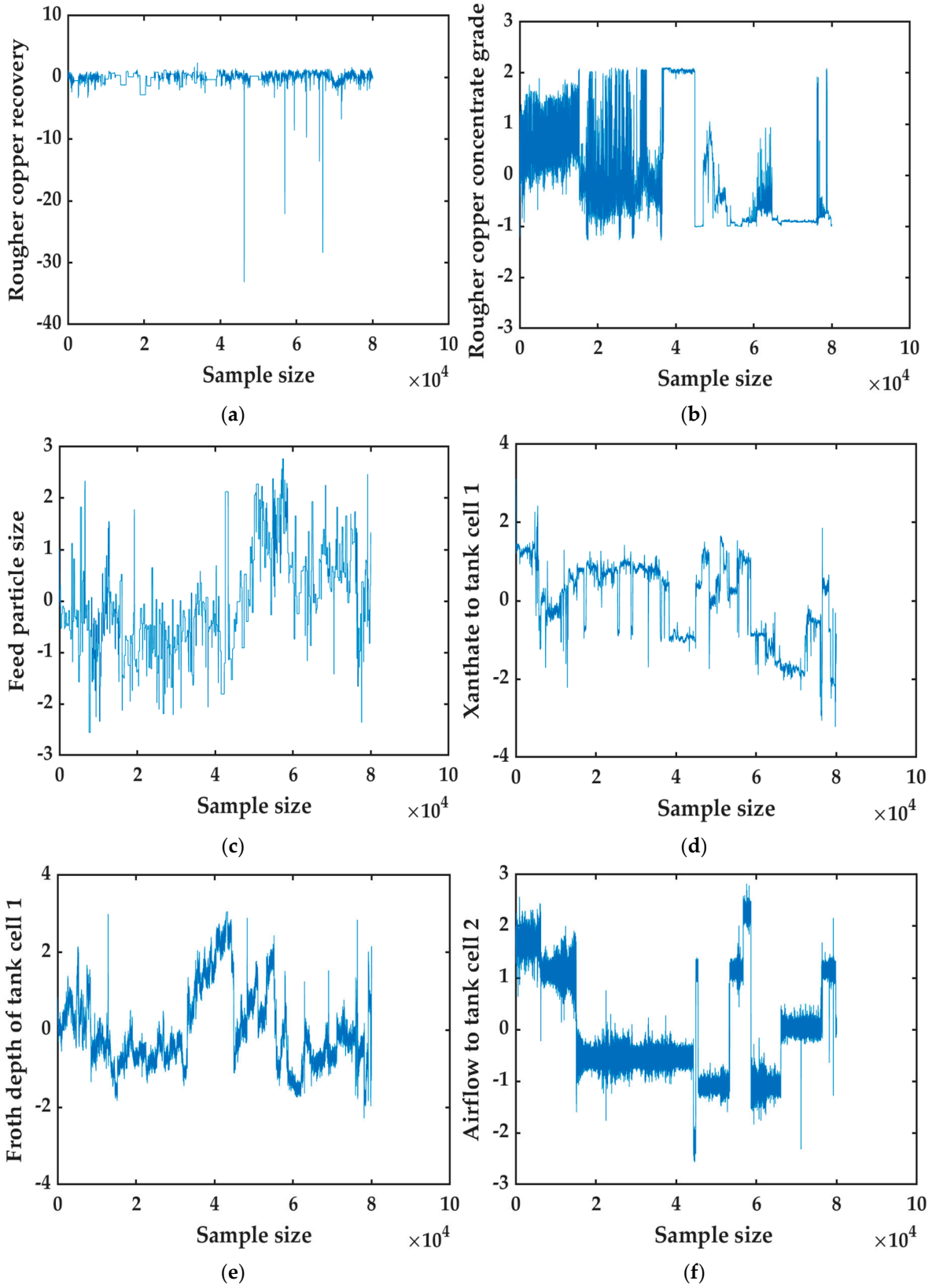

Figure 1. Variation in (**a**) copper recovery; (**b**) concentrate copper grade; (**c**) particle size; (**d**) xanthate dosage to tank cell 1; (**e**) froth depth of tank cell 1; and (**f**) airflow to tank cell 2.

2.2. Model Development and Evaluation

For the GPR predictive model development, a portion of the pre-processed data set (30,000 observations) was sampled randomly from 74,633 observations for model training and validation owing to the expensive computational time accompanying a large data set. The required size of the sampled data set was ascertained from an empirical study, which revealed the saturation of the model performance after 30,000 observations. Furthermore, the sampling was repeated until the sample and population statistics (mean, median, minimum, and maximum values) difference were below 5%. Following this, the sampled data set was randomly partitioned into 80% training data (24,000 observations) and 20% validation data (6000 observations), based on the holdout cross-validation technique [35]. It must be noted that the partitioning ratio does not follow a particular rule, but generally, the training data should completely capture the population data. The remaining portion of the pre-processed data set (44,663 observations) served as the testing data set. In the GPR algorithm, the main hyperparameter that affects the performance of the algorithm is the covariance function. In this regard, this work utilised four covariance functions (rational quadratic, squared exponential, exponential, and matern 3/2) in the modelling of each output variable. The mathematical expressions of these covariance functions are shown in Equations (3)–(6).

i. Squared exponential covariance function

$$k(x_i,\ x_j) = \sigma_f^2 \exp\left[\frac{-d^2}{2l^2}\right]; \tag{3}$$

ii. Rational quadratic covariance function

$$k(x_i,\ x_j) = \sigma_f^2 \exp\left[1 + \frac{d^2}{2\alpha l^2}\right]^{-\alpha}; \tag{4}$$

iii. Exponential covariance function

$$k(x_i, x_j) = \sigma_f^2 \exp\left[\frac{-d}{l}\right]; \tag{5}$$

iv. Matern 3/2 covariance function

$$k(x_i, x_j) = \sigma_f^2 \left(1 + \frac{\sqrt{3}d}{l}\right) \exp\left(-\frac{\sqrt{3}d}{l}\right); \tag{6}$$

where the Euclidean distance between x_i *and* $x_j, d = \sqrt{\left(x_i - x_j\right)'\left(x_i - x_j\right)}$, σ_f^2 is the signal variance of the function, α is the shape parameter for the rational quadratic covariance function, and l is the length scale. In previous research using the GPR model on the input variables, the percent particle size passing 75 µm variable contributed more than the other variables [17].

Having prior knowledge about the outcome (recovery and grade) of a flotation process will continue to be of great interest to the process engineer. The accuracy of the various developed GPR models were assessed by the mean absolute percentage error (MAPE), the correlation coefficient (r), the relative root mean square error (RRMSE), and the relative error correction (REC). The various mathematical notations are presented in Equations (7)–(10). For a good performance under the following indicators, the models' r values should approach 1, and the MAPE and RRMSE values should be close to zero with REC as close to 100% as possible.

$$r = \frac{\sum_{i=1}^{n} (y_i - \overline{y}) - (\hat{y}_i - \overline{\hat{y}})}{\sum_{i=1}^{n} (y_i - \overline{y})^2 \times \sqrt{\sum_{i=1}^{n} (\hat{y}_i - \overline{\hat{y}})^2}} \tag{7}$$

$$\text{MAPE} = \left(\frac{1}{n}\right)\sum_{i=1}^{n}\frac{|y_i - \hat{y}_i|}{y_i} \times 100\% \quad (8)$$

$$\text{RRMSE} = \frac{\sqrt{\left(\frac{1}{n}\right)\sum_{i=1}^{n}(y_i - \hat{y}_i)^2}}{\frac{1}{n}\sum_{i=1}^{n}\hat{y}_i} \quad (9)$$

$$\text{REC} = 100 - \left(\frac{100}{n}\sum_{i=1}^{n}\frac{|y_i - \hat{y}_i|}{y_i}\right), \quad (10)$$

where

$y_i = i$th true copper recovery or copper-concentrate grade value;
$\overline{y}$ = mean of true copper recovery or copper-concentrate grade values;
$\hat{y}_i = i$th predicted copper recovery or copper-concentrate grade value;
$\overline{\hat{y}}$ = mean of predicted copper recovery or copper-concentrate grade value;
n = total number of observations.

2.3. Optimisation Modelling

Problem Formulation

Using the predictive functions of the best performing copper recovery and concentrate grade models as the objective functions, the multiobjective optimisation of various rougher flotation variables that maximises both the copper recovery and concentrate grade were carried out using the controlled-NSGA-II and PA. The problem formulation is shown in Equation (11). A theoretical overview of the pareto search algorithm and the controlled-NSGA-II has been previously reported; hence, it is not repeated here [36,37] Custódio, Madeira [38].

$$\begin{cases} \textit{Maximise (Copper recovery)} \\ \textit{Maximise (Copper concentrate grade)} \end{cases} \quad (11)$$

such that

1.6 w.t%$\leq$ *feed grade* $\leq$ 2.6 w.t%;
78.0% $\leq$ *Feed particle size* $\leq$ 84.0%;
350.0 t/h $\leq$ *Throughput* $\leq$ 900.0 t/h;
37.0 mL/min $\leq$ *Xanthate to tank cell* 1 $\leq$ 190.5 mL/min;
27.8 mL/min $\leq$ *Xanthate to tank cell* 4 $\leq$ 142.9 mL/min;
28.1 mL/min $\leq$ *Frother to tank cells* 1 *and* 4 $\leq$180.7 mL/min;
900.0 m^3/h $\leq$ *Airflow to tank cell* 1 $\leq$ 1250.0 m^3/h;
1100.0 m^3/h $\leq$ *Airflow to tank cells* 2, 3, 4 *and* 5 $\leq$ 1250.0 m^3/h;
75.0 mm $\leq$ *Froth depth of tank cell* 1, 2, 3, 4 *and* 5 $\leq$ 150.0 mm.

These boundary constraints were developed based on the domain knowledge of the process conditions.

3. Results and Discussion

In this section, results from the various techniques are presented and discussed. In Section 3.1, discussion of the different GPR models from different covariance functions is presented. Section 3.2 details the comparative results of the MO algorithms.

3.1. Predictive Models' Performance

In the prediction of the copper recovery and concentrate grade, the GPR models with four covariance functions were developed assuming the two output variables were independent of each other. The prediction of each output variable was evaluated by considering the predicted and actual values. This evaluation was accurately carried out

using *r*, MAPE, RRMSE, and REC criteria. The summary results of the developed models are shown in Table 1.

Table 1. Summary of the GPR models' performance for copper recovery prediction.

Training Data Set				
GPR Covariance Function	***r***	**MAPE (%)**	**RRMSE**	**REC (%)**
Squared exponential	0.95	0.04	0.03	99.80
Rational quadratic	0.99	0.02	0.01	99.98
Exponential	0.97	0.02	0.02	99.96
Matern 3/2	0.95	0.03	0.04	99.78
Validation Data Set				
GPR Covariance Function	***r***	**MAPE (%)**	**RRMSE**	**REC (%)**
Squared exponential	0.94	0.29	0.46	83.83
Rational quadratic	0.96	0.24	0.38	85.47
Exponential	0.96	0.28	0.42	84.28
Matern 3/2	0.95	0.30	0.46	83.80
Testing Data Set				
GPR Covariance Function	***r***	**MAPE (%)**	**RRMSE**	**REC (%)**
Squared exponential	0.95	0.33	0.42	84.10
Rational quadratic	0.97	0.26	0.37	85.39
Exponential	0.96	0.30	0.44	83.98
Matern 3/2	0.97	0.33	0.43	83.97

Considering Table 1, the GPR model from the rational quadratic covariance function had a relatively better performance than all the other models and was therefore considered to be the best model for the prediction of rougher copper recovery. Correlation coefficient values of 0.99, 0.96, and 0.97 were observed, respectively, for the training data, validation data, and testing data when the rational quadratic covariance function was used. These values show a clear indication of the strong relationship between the actual and predicted recovery values under the rational quadratic covariance function.

For error statistics, the MAPE and RRMSE were considered in this work. The trained GPR model developed with rational quadratic covariance function had MAPE values of 0.02%, 0.24%, and 0.26% when rougher copper recovery was predicted using the training, validation, and testing data sets, respectively. On average, these recorded MAPE values indicate that GPR model developed with the rational quadratic covariance function was distant by 0.02%, 0.24%, and 0.26% from the actual training, validation, and testing recovery values, respectively. With regard to the MAPE, the GPR model developed with the rational quadratic covariance function was able to explain 99.98%, 99.76%, and 99.74% of the total useful recovery information in the training, validation, and testing data, respectively. The low MAPE values of the rational quadratic covariance function shows its higher prediction accuracy than all the other investigated covariance functions in predicting rougher copper recovery.

In terms of the RRMSE, the results of the various GPR models shown in Table 1 indicate that all the models had a very satisfactory rougher copper recovery prediction. However, the rational quadratic covariance function had the best performance obtaining RRMSE values of 0.01 (training data), 0.38 (validation data), and 0.37 (testing data).

In general, the REC reveals the percent closeness of the data to the best fit line. From Table 1, the GPR model developed with the rational quadratic covariance function recorded the highest REC values of 99.98% (training data), 85.47% (validation data), and 85.39%

(testing data), confirming their close association with their actual copper recovery values. This close association obtained by the GPR model developed with the rational quadratic covariance function is visualised in Figure 2. Comparing these results to previous work, as highlighted in Section 2.1, it can be seen that similar results were obtained even though different year ranges of the data set were considered in each case.

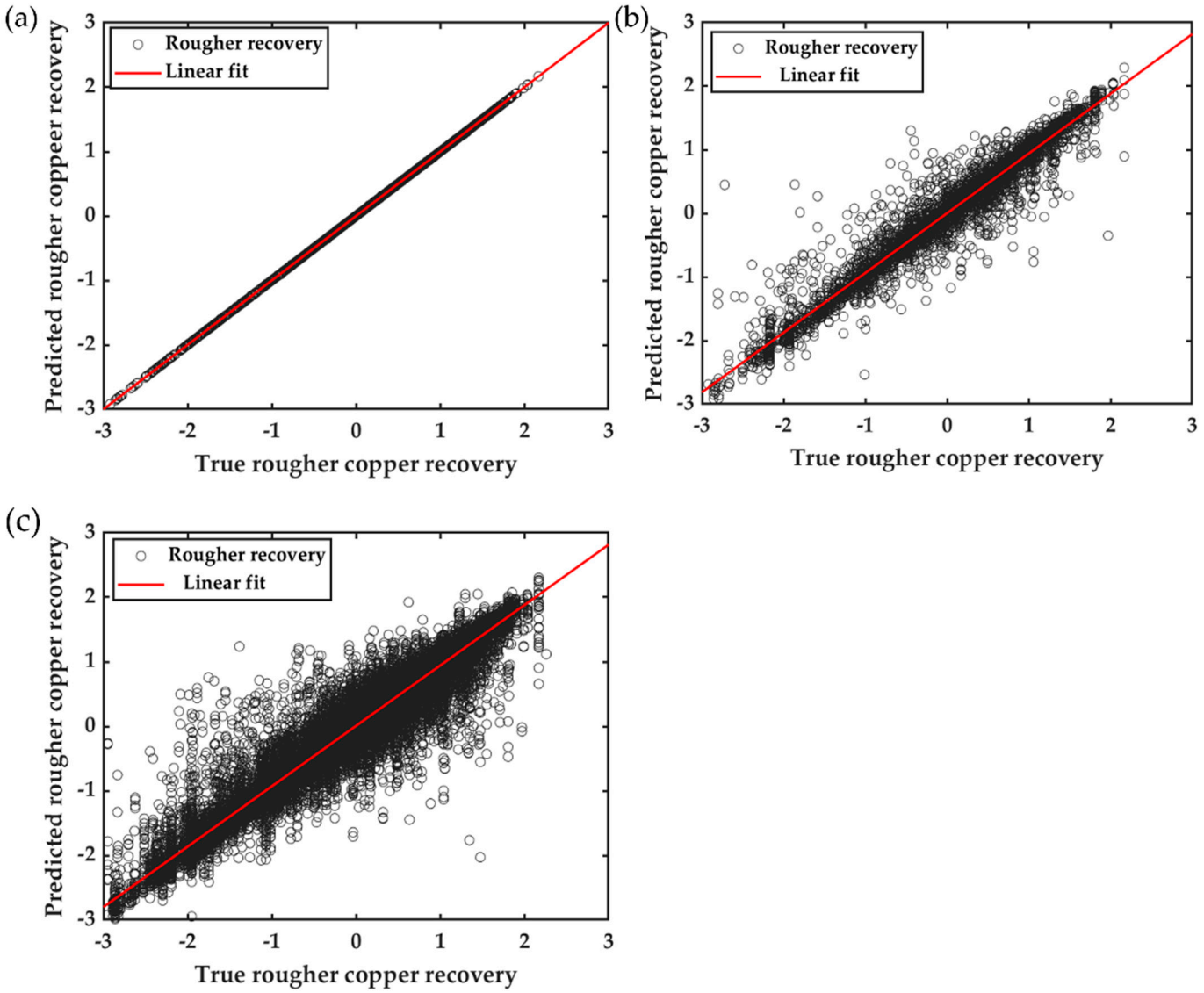

Figure 2. Visualisation of the actual (true) and predicted copper recovery for the (**a**) training data set; (**b**) validation data set; and (**c**) testing data set using the GPR rational quadratic covariance model.

The prediction of the concentrate grade was also determined utilising the same GPR covariance functions highlighted above. The performances of the various GPR models are shown in Table 2. It is evident that the development of the GPR model using the matern 3/2 covariance function marginally outperformed the other investigated models making it the best model in the prediction of the rougher concentrate copper grade. Referring to Table 2, the r values > 0.97, the MAPE values < 0.18%, the RRMSE < 0.27, and the REC values > 92% were recorded for the matern 3/2 covariance model. The covariance functions' copper recovery and concentrate grade predictive performance differences are due to the fact that during the transformation of the data set into higher dimensional space for the unique discrimination of the labels, the transformations conducted by these covariance functions (rational quadratic for rougher copper recovery and Matern 3/2 for rougher

copper concentrate grade) had a better higher dimensional space correlation structure between the output variables and input variables as compared to the other covariance functions investigated in this work.

Table 2. Summary of the models' performance for the prediction of the rougher copper concentrate grade.

Training Data Set				
GPR Covariance Function	***r***	**MAPE (%)**	**RRMSE**	**REC (%)**
Squared exponential	0.96	0.02	0.02	99.95
Rational quadratic	0.98	0.02	0.01	99.97
Exponential	0.97	0.02	0.01	99.97
Matern 3/2	0.99	0.01	0.01	99.99
Validation Data Set				
GPR Covariance Function	***r***	**MAPE (%)**	**RRMSE**	**REC (%)**
Squared exponential	0.97	0.19	0.29	91.81
Rational quadratic	0.98	0.18	0.27	91.86
Exponential	0.97	0.19	0.28	91.82
Matern 3/2	0.98	0.17	0.25	92.92
Testing Data Set				
GPR Covariance Function	***r***	**MAPE (%)**	**RRMSE**	**REC (%)**
Squared exponential	0.97	0.23	0.28	92.20
Rational quadratic	0.97	0.21	0.29	91.95
Exponential	0.98	0.19	0.28	92.56
Matern 3/2	0.99	0.16	0.26	92.99

Furthermore, comparing the results in Tables 1 and 2 generally shows that the overall concentrate grade prediction accuracy is marginally better than that of the rougher copper recovery. This is expected because as compared to the rougher copper recovery, the rougher copper concentrate grade had a lower range of values giving it more instances per label and therefore an easier characterisation. Just like the recovery prediction, Figure 3 shows the closeness between actual and predicted concentrate grade under the GPR matern 3/2 covariance model.

Based on the above discussion, the best performing predictive function in each instance was extracted as the objective function for the flotation variables optimisation that would maximise both the rougher copper recovery and the rougher copper concentrate grade.

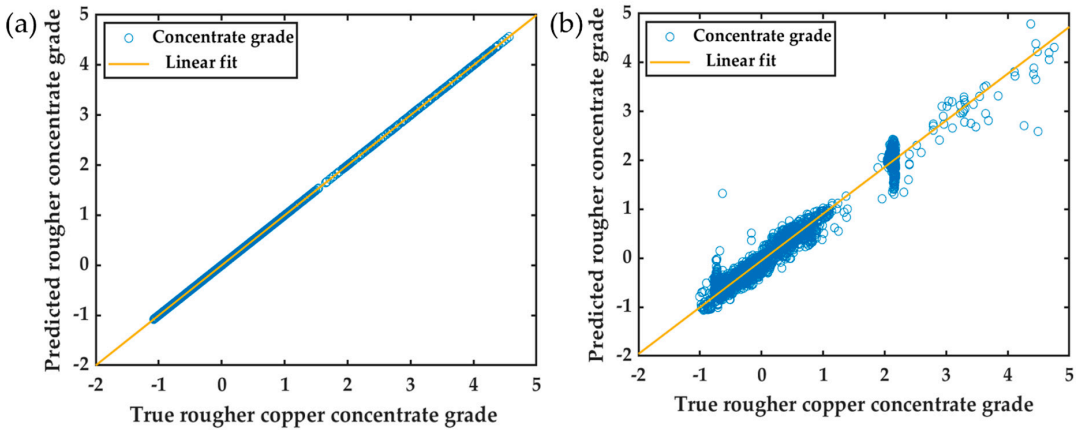

Figure 3. *Cont.*

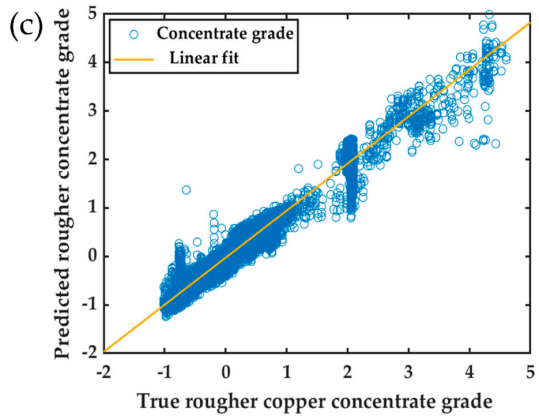

Figure 3. Visualisation of the actual (true) and predicted concentrate grade values for the (**a**) training data set (**b**) validation data set, and (**c**) testing data set using the GPR matern 3/2 covariance model.

3.2. Best Multiobjective Algorithm Selection

The optimisation capability of the PA and controlled-NSGA-II has been evaluated. A total of 70 sets of pareto-optimal solutions were investigated for each algorithm. Out of these, four pareto-optimal solutions were further explored for each algorithm based on a rougher copper recovery constraint of at least 93% at a satisfactory grade. Figure 4 visualises the optimal solutions found by the PA and controlled-NSGA-II.

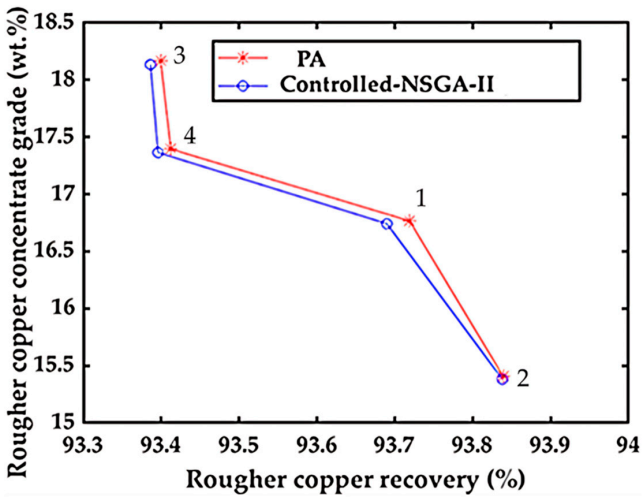

Figure 4. Visualisation of the solutions from the PA and controlled-NSGA-II. The solutions, corresponding to those shown in Table 3, are labelled from 1 to 4.

Table 3. Pareto-optimal solutions found by PA. * Froth depth of tank cells 2 and 4 represent tank cells 3 and 5, respectively.

Variable		Solution 1	Solution 2	Solution 3	Solution 4
Flotation feed grade (wt.%)		2.52	1.60	2.52	2.52
Percent particle passing 75 µm		78.00	80.22	78.00	78.00
Mill throughput (t/h)		600.00	670.56	679.69	679.69
Xanthate dosage in tanks 1 and 4 (ml/min)	1	69.11	66.98	190.50	69.11
	4	29.93	27.80	29.93	29.93
Frother dosage in tanks 1 and 4 (ml/min)	1	40.94	38.81	40.94	40.94
	4	28.10	28.10	28.10	28.10

Table 3. *Cont.*

Variable		Solution 1	Solution 2	Solution 3	Solution 4
Air flow rate in tanks 1 to 5 (m^3/h)	1	1215.63	1213.49	1215.63	900.00
	2	1195.00	1192.87	1195.00	1195.00
	3	1165.63	1163.49	1165.63	1165.63
	4	1212.50	1210.37	1212.50	1212.50
	5	1100.00	1100.00	1100.00	1100.00
Froth depth in tanks 1 to 5 (mm)	1	150.00	150.00	150.00	150.00
	2/3 *	135.35	133.22	135.35	135.35
	4/5 *	150.00	150.00	150.00	150.00
Copper recovery (%)		93.72	93.84	93.40	93.41
Concentrate copper grade (wt.%)		16.77	15.41	18.16	17.40

From Figure 4, it is evident that the optimal solutions from the PA and controlled-NSGA-II are very similar. However, comparing the two algorithms, the pareto-optimal solutions found by the PA lies marginally above that of the controlled-NSGA-II, making it a better technique for this work. As such, only the pareto-optimal solutions found by the PA will be further discussed.

Selection of the Best Solution

The PA optimal solutions are shown in Table 3. The results from Table 3 clearly indicate that there is an inverse relationship between the rougher copper recovery and the rougher copper concentrate grade. In other words, the conditions that maximise the rougher copper recovery are the same conditions that minimise the rougher copper concentrate grade. Therefore, to select the best set of pareto-optimal solutions, there should be a proper trade-off between the rougher copper recovery and rougher copper concentrate grade, with an emphasis on variables that have a significant economic impact on the process. In this work, emphasis was placed on the throughput, xanthate dosage, feed particle size, and frother dosages.

From Table 3, solutions 1, 3, and 4 had a comparatively coarse grinding of 78% passing 75 µm making them better options over solution 2, with regard to the feed particle size. In terms of the throughput, solution 1 had the least tonnages of material treated per hour followed by solution 2, with solutions 3 and 4 recording the same throughput of almost 680 t/h. At this stage, it can be seen that the best set of solutions lies between solutions 3 and 4, as they have the same feed particle size and throughput. It is worth noting that despite the lower feed grade of solution 2, the recovery was subtly higher than the other solutions. The higher recovery value may be due to the corresponding finer grind, with the low feed grade also contributing to a lower concentrate grade relative to the other solutions [39,40]. With the equivalent performance of solutions 3 and 4, their reagent consumptions (xanthate and frother dosages) were assessed. Again, from Table 3, solutions 3 and 4 had the same reagent consumptions except for the xanthate consumption in tank cell 1, where solution 3 consumed almost thrice the quantity of xanthate of solution 4. With similar rougher copper recovery values of 93.40% and 93.41% attained by solutions 3 and 4, respectively, it can be observed that solution 3 had a higher rougher copper concentrate grade of 18.16 wt.% as compared to solution 4, which had 17.40 wt.%. However, the argument is that the difference in the rougher copper concentrate grade will not be enough to compensate for the xanthate cost, which may have contributed to the higher grade, if the processing plant is to be run with solution 3 [41–44]. Moreover, the concentrate obtained at the roughing stage will further undergo upgrade during the cleaning stage and that is why emphasis is often placed on the recovery over the concentrate grade during the roughing

stage. Based on the above analysis, solution 4 was selected as the best set of pareto-optimal solutions in this work.

In as much as the optimum operating values have been determined for the various rougher flotation variables, variables like the throughput, feed grade, and feed particle size often vary simultaneously and are very difficult to maintain at a particular set point in a typical industrial operation. Two of these variables (feed grade and feed particle size) have been further analysed to ascertain the simultaneous impact of a varying feed grade and feed particle size on the copper recovery and concentrate grade. To accomplish this, 50 typical industrial observations of feed grade and feed particle size were generated within their specified constraint bounds shown in Equation (10), having all possible generated combinations of the initial feed grade and particle size observations to yield 2500 observations for the two variables. Now, varying the feed grade and particle size simultaneously, while maintaining the other variables at optimum operating points, the best performing predictive models were used to simulate both the rougher copper recovery and rougher copper concentrate grade. The simulation results are visualised in Figure 5. From Figure 5a, it is evident that an increasing feed grade with a decreasing feed particle size enhances the rougher copper recovery and vice versa. The increase in rougher copper recovery occurs as a result of the larger exposure of the copper mineral surface for reagent contact, with a finer grind. However, this phenomenon is not the same with the rougher copper concentrate grade, as shown in Figure 5b. From Figure 5b, an increasing feed grade with a decreasing feed particle size decreases the rougher copper concentrate grade and vice versa. The rougher copper concentrate grade decreases because fine grinding activates the surfaces of other gangue minerals leading to their floatability and subsequent dilution of the rougher copper concentrate grade. Whereas certain combinations of feed particle size and feed grade in their specified constraint bounds are likely to reduce the predicted copper recovery and concentrate grade, the grade and recovery values within the range of 15.70–17.40 wt.% and 93.36–93.48%, respectively, are still attainable when all the other variables are kept at their optimum points. With much emphasis on recovery during the roughing stage, the results affirm that a near optimal rougher copper recovery at a satisfactory grade is achievable within the specified feed grade and particle size constraint bounds when the other variables are kept at their ascertained optimum points.

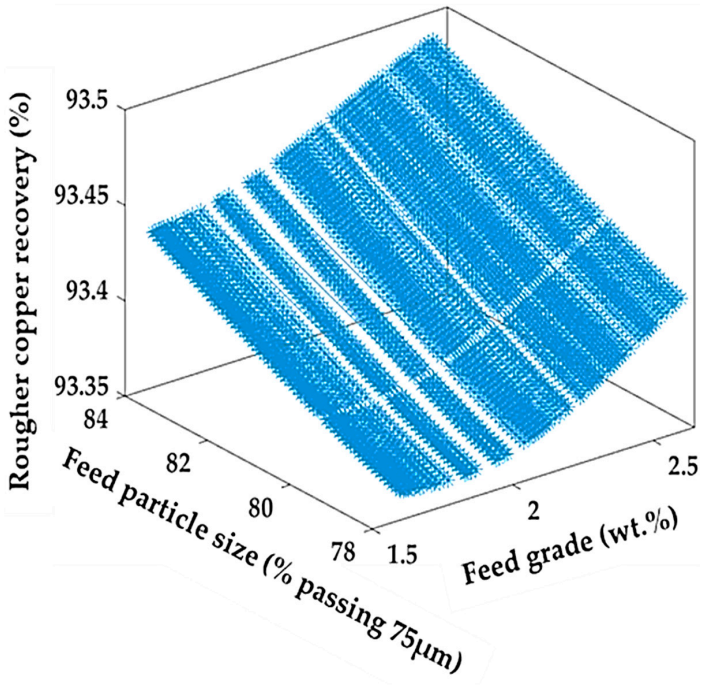

(**a**)

Figure 5. *Cont.*

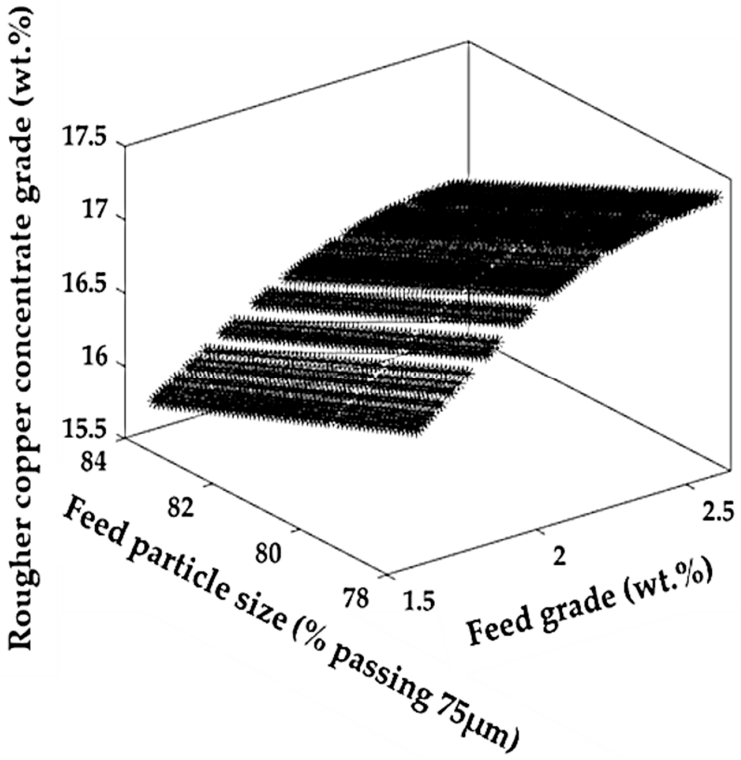

(**b**)

Figure 5. Visualising the simultaneous feed particle size and feed grade variation on the (**a**) copper recovery and (**b**) concentrate copper grade.

4. Conclusions

In this work, Gaussian process regression (GPR) models developed under different covariance functions have been used in copper recovery and concentrate copper grade prediction. Following this, the predictive functions of the best models (covariance type) ascertained during the prediction of each output variable were extracted as the objective functions. Using these two objective functions subjected to some process constraints, the PA and controlled-NSGA-II were used to investigate the optimum variable conditions that would maximise both the copper recovery and concentrate copper grade. The main conclusions are as follows:

(1) The model assessment showed good copper recovery and concentrate grade prediction from the flotation variables using the GPR model.
(2) The rational quadratic covariance function worked best for copper recovery prediction, while the matern 3/2 covariance function worked best for the concentrate copper grade prediction.
(3) The comparison between the PA and controlled-NSGA-II revealed that the PA, although the controlled-NSGA-II also worked very well, finds the best set of pareto-optimal solutions for both the copper recovery and concentrate grade maximisation.
(4) Selecting a final optimal solution requires domain knowledge. For example, the optimal solution for the rougher flotation stage (focussed on maximising the throughput) may differ from that of the cleaner flotation stage (focus may be on higher product grades).
(5) Further analysis of the best set of pareto-optimal solutions also revealed that a near optimal rougher copper recovery at a satisfactory grade is still attainable with varying feed grades and particle sizes when all the other flotation variables are kept at their optimum values.

The significance of this work is that the developed models could be used to simulate both copper recovery and concentrate in a mineral processing plant following similar

conditions. Moreover, operating the rougher circuit at the suggested optimum points would result in a more stabilised flotation performance.

Author Contributions: Conceptualization, B.A.-K. and R.K.A.; methodology, B.A.-K. and R.K.A.; validation, B.A.-K., C.M. and R.K.A.; formal analysis, B.A.-K. and R.K.A.; investigation, B.A.-K.; resources, B.A.-K., C.M., K.E. and R.K.A.; data curation, B.A.-K.; writing—original draft preparation, B.A.-K.; writing—review and editing, B.A.-K., C.M., K.E. and R.K.A.; visualization, B.A.-K.; supervision, C.M., K.E. and R.K.A.; project administration, K.E. and R.K.A.; funding acquisition, R.K.A. All authors have read and agreed to the published version of the manuscript.

Funding: This research has been supported by the South Australian Government through the PRIF RCP Industry Consortium, providing research scholarship to the first author (B.A.-K.). The authors thank BHP Olympic Dam for approving the publication of this article. Financial support from the Future Industries Institute of the University of South Australia is also acknowledged.

Data Availability Statement: Confidential data is not available.

Acknowledgments: Support from the Australia–India Strategic Research Fund for the Recovery of the Battery Materials and REE from Ores and Wastes is also acknowledged. Support from the Australian Research Council Centre for Excellence for Enabling Eco-Efficient Beneficiation of Minerals (grant number CE200100009) is gratefully acknowledged.

Conflicts of Interest: Conor McCamley is an employee of Syrah Resources, and Kathy Ehrig is an employee of BHP. The remaining authors declare that the research was conducted in the absence of any commercial or financial relationships that could be construed as a potential conflict of interest.

References

1. Gharai, M.; Venugopal, R. Modeling of Flotation Process—An Overview of Different Approaches. *Miner. Process. Extr. Metall. Rev.* **2016**, *37*, 120–133. [CrossRef]
2. Jovanović, I.; Miljanović, I.; Jovanović, T. Soft computing-based modeling of flotation processes—A review. *Miner. Eng.* **2015**, *84*, 34–63. [CrossRef]
3. Quintanilla, P.; Neethling, S.J.; Brito-Parada, P.R. Modelling for froth flotation control: A review. *Miner. Eng.* **2021**, *162*, 106718. [CrossRef]
4. Jahedsaravani, A.; Marhaban, M.H.; Massinaei, M. Application of Statistical and Intelligent Techniques for Modeling of Metallurgical Performance of a Batch Flotation Process. *Chem. Eng. Commun.* **2016**, *203*, 151–160. [CrossRef]
5. Hayat, M.B. *Mitigation of Environmental Hazards of Sulfide Mineral Flotation with an Insight into Froth Stability and Flotation Performance*; Missouri University of Science and Technology: Rolla, MO, USA, 2018.
6. Wang, G.; Nguyen, A.V.; Mitra, S.; Joshi, J.B.; Jameson, G.J.; Evans, G.M. A review of the mechanisms and models of bubble-particle detachment in froth flotation. *Sep. Purif. Technol.* **2016**, *170*, 155–172. [CrossRef]
7. Yoon, R.-H.; Soni, G.; Huang, K.; Park, S.; Pan, L. Development of a turbulent flotation model from first principles and its validation. *Int. J. Miner. Process.* **2016**, *156*, 43–51. [CrossRef]
8. Chilliers, J.J.; Asplin, R.A.; Woodburn, E.T. Kinetic Flotation Modelling Using Froth Imaging Data. In *Frothing in Flotation*; Woodburn, E.T., Ed.; Routledge: Boca Raton, FL, USA, 1998; pp. 309–335. [CrossRef]
9. Feng, Q.; Zhang, J.; Zhang, X.; Wen, S. Proximate analysis based prediction of gross calorific value of coals: A comparison of support vector machine, alternating conditional expectation and artificial neural network. *Fuel Process. Technol.* **2015**, *129*, 120–129. [CrossRef]
10. Khodakarami, M.; Molatlhegi, O.; Alagha, L. Evaluation of ash and coal response to hybrid polymeric nanoparticles in flotation process: Data analysis using self-learning neural network. *Int. J. Coal Prep. Util.* **2019**, *39*, 199–218. [CrossRef]
11. Zarie, M.; Jahedsaravani, A.; Massinaei, M. Flotation froth image classification using convolutional neural networks. *Miner. Eng.* **2020**, *155*, 106443. [CrossRef]
12. Amankwaa-Kyeremeh, B.; Greet, C.J.; Skinner, W.; Zanin, M.; Asamoah, R.K. Selecting key predictor parameters for regression analysis using modified neighbourhood componenet analysis (NCA) algorithm. In Proceedings of the 6th UMaT Biennial International Mining and Mineral Conference, Tarkwa, Ghana, 5–6 August 2020; pp. 320–325.
13. Jahedsaravani, A.; Marhaban, M.; Massinaei, M. Prediction of the metallurgical performances of a batch flotation system by image analysis and neural networks. *Miner. Eng.* **2014**, *69*, 137–145. [CrossRef]
14. Jahedsaravani, A.; Marhaban, M.; Massinaei, M.; Saripan, M.; Noor, S. Froth-based modeling and control of a batch flotation process. *Int. J. Miner. Process.* **2016**, *146*, 90–96. [CrossRef]
15. Amankwaa-Kyeremeh, B.; Greet, C.; Zanin, M.; Skinner, W.; Asamoah, R.K. Predictability of rougher flotation copper recovery using Gaussian process regression algorithm. In Proceedings of the 6th UMaT Biennial International Mining and Mineral Conference, Tarkwa, Ghana, 5–6 August 2020; Ghana UMaT: Tarkwa, Ghana, 2020; pp. 1–8.

16. Yang, K.; Jin, H.; Chen, X.; Dai, J.; Wang, L.; Zhang, D. Soft sensor development for online quality prediction of industrial batch rubber mixing process using ensemble just-in-time Gaussian process regression models. *J. Chemom. Intell. Lab. Syst.* **2016**, *155*, 170–182. [CrossRef]
17. Amankwaa-Kyeremeh, B.; Zhang, J.; Zanin, M.; Skinner, W.; Asamoah, R.K. Feature selection and Gaussian process prediction of rougher copper recovery. *Miner. Eng.* **2021**, *170*, 107041. [CrossRef]
18. Amankwaa-Kyeremeh, B.; Greet, C.; Skinner, W.; Asamoah, R.K. Correlating process mineralogy and pulp chemistry for quick ore variability diagnosis. In Proceedings of the International Future Mining Conference, Online, 6–10 December 2021; Australia Australia Australasian Institute of Mining and Metallurgy: Carlton, Australia, 2021; pp. 1–10.
19. Patel, A.K.; Gorai, A.K.; Chatterjee, S. Development of Machine vision-based system for iron ore grade prediction using Gaussian Process Regression (GPR). In Proceedings of the Pattern Recognition and Information processing (PRIP'2016), Minsk, Belarus, 3–5 October 2016; pp. 45–48.
20. Arthur, C.K.; Temeng, V.A.; Ziggah, Y.Y. Novel approach to predicting blast-induced ground vibration using Gaussian process regression. *Eng. Comput.* **2020**, *36*, 29–42. [CrossRef]
21. Amankwaa Kyeremeh, B.; Ehrig, K.; Greet, C.; Asamoah, R. Pulp chemistry variables for gaussian process prediction of rougher copper recovery. *Minerals* **2023**, *13*, 731. [CrossRef]
22. Amankwaa-Kyeremeh, B.; McCamley, C.; Zanin, M.; Greet, C.; Ehrig, K.; Asamoah, R.K. Prediction and Optimisation of Copper Recovery in the Rougher Flotation Circuit. *Minerals* **2024**, *14*, 36. [CrossRef]
23. Amankwaa-Kyeremeh, B.; Skinner, W.; Asamoah, R.K. Comparative study on rougher copper recovery prediction using selected predictive algorithms. In Proceedings of the International Future Mining Conference, Sydney, Australia, 6–10 December 2021; Australia Australia Australasian Institute of Mining and Metallurgy: Carlton, Australia, 2021; pp. 1–10.
24. Cook, R.; Monyake, K.C.; Hayat, M.B.; Kumar, A.; Alagha, L. Prediction of flotation efficiency of metal sulfides using an original hybrid machine learning model. *Eng. Rep.* **2020**, *2*, e12167. [CrossRef]
25. Weichert, D.; Link, P.; Stoll, A.; Rüping, S.; Ihlenfeldt, S.; Wrobel, S. A review of machine learning for the optimization of production processes. *Int. J. Adv. Manuf. Technol.* **2019**, *104*, 1889–1902. [CrossRef]
26. Schmidt, J.; Marques, M.R.; Botti, S.; Marques, M.A. Recent advances and applications of machine learning in solid-state materials science. *Comput. Mater.* **2019**, *5*, 83. [CrossRef]
27. Müller, J. MISO: Mixed-integer surrogate optimization framework. *Optim. Eng.* **2016**, *17*, 177–203. [CrossRef]
28. Yu, D.; Hong, J.; Zhang, J.; Niu, Q. Multi-objective individualized-instruction teaching-learning-based optimization algorithm. *Appl. Soft Comput.* **2018**, *62*, 288–314. [CrossRef]
29. Wang, S.; Zhao, D.; Yuan, J.; Li, H.; Gao, Y. Application of NSGA-II algorithm for fault diagnosis in power system. *Electr. Power Syst. Res.* **2019**, *175*, 105893. [CrossRef]
30. Beirigo, B.A.; dos Santos, A.G. Application of NSGA-II framework to the travel planning problem using real-world travel data. In Proceedings of the 2016 IEEE Congress on Evolutionary Computation (CEC), Vancouver, BC, Canada, 24–29 July 2016; pp. 746–753.
31. Gantayet, A.; Dheer, D.K. Multiobjective Planning Strategy for a Distribution Network integrated with Wind Power System considering Solid State Transformer. In Proceedings of the 2021 International Conference on Computational Performance Evaluation (ComPE), Shillong, India, 1–3 December 2021; pp. 692–697.
32. Mišo, B.B.; Branko, S.R.; Kolarik, L.; Petrovic, A.V. Multi-objective calibration of the double-ellipsoid heat source model for gmaw process simulation. *Therm. Sci.* **2022**, *26*, 2081–2092.
33. Arthur, C.K.; Kaunda, R.B. A hybrid paretosearch algorithm and goal attainment method for maximizing production and reducing blast-induced ground vibration: A blast design parameter selection approach. *Min. Technol.* **2020**, *129*, 151–158. [CrossRef]
34. Ehrig, K.; McPhie, J.; Kamenetsky, V. Geology and mineralogical zonation of the Olympic Dam iron oxide Cu-U-Au-Ag deposit, South Australia. In *Geology and Genesis of Major Copper Deposits and Districts of the World, a Tribute to Richard Sillitoe*; Hedenquist, J.W., Harris, M., Camus, F., Eds.; Society of Economic Geologists Inc.: Littleton, CO, USA, 2012; Volume 16, pp. 237–268.
35. Raschka, S. Model evaluation, model selection, and algorithm selection in machine learning. *arXiv* **2018**, arXiv:1811.12808.
36. Bratley, P.; Fox, B.L. Algorithm 659: Implementing Sobol's quasirandom sequence generator. *ACM Trans. Math. Softw.* **1988**, *14*, 88–100. [CrossRef]
37. Fleischer, M. The measure of Pareto optima applications to multi-objective metaheuristics. In Proceedings of the International Conference on Evolutionary Multi-Criterion Optimization, Faro, Portugal, 8–11 April 2003; pp. 519–533.
38. Custódio, A.L.; Madeira, J.A.; Vaz, A.I.F.; Vicente, L.N. Direct multisearch for multiobjective optimization. *SIAM J. Optim.* **2011**, *21*, 1109–1140. [CrossRef]
39. Owusu, K.B.; Karageorgos, J.; Greet, C.; Zanin, M.; Skinner, W.; Asamoah, R.K. Predicting mill feed grind characteristics through acoustic measurements. *Miner. Eng.* **2021**, *171*, 107099. [CrossRef]
40. Asamoah, R.K.; Baawuah, E.; Greet, C.; Skinner, W. Characterisation of metal debris in grinding and flotation circuits. *Miner. Eng.* **2021**, *171*, 107074. [CrossRef]
41. Forson, P.; Zanin, M.; Abaka-Wood, G.; Skinner, W.; Asamoah, R. Flotation of auriferous arsenopyrite from pyrite using thionocarbamate. *Miner. Eng.* **2022**, *181*, 107524. [CrossRef]
42. Forson, P.; Skinner, W.; Asamoah, R. Investigating the selective flotation of auriferous arsenian pyrite from refractory ores using thionocarbamate. *Powder Technol.* **2023**, *426*, 118649. [CrossRef]

43. Dankwah, J.B.; Asamoah, R.K.; Zanin, M.; Skinner, W. Dense liquid flotation: Can coarse particle flotation performance be enhanced by controlling fluid density? *Miner. Eng.* **2022**, *180*, 107513. [CrossRef]
44. Forson, P.; Zanin, M.; Skinner, W.; Asamoah, R. Differential flotation of pyrite and Arsenopyrite: Effect of pulp aeration and the critical importance of collector concentration. *Miner. Eng.* **2022**, *178*, 107421. [CrossRef]